Polymer 50 (2009) 2793–2805

Contents lists available at ScienceDirect

Polymer

journal homepage: www.elsevier.com/locate/polymer

Synthesis and properties of chiral helical polymers based on optically active polybinaphthyls

Xiaobo Huang [a,b], Ying Xu [a], Qian Miao [b], Lili Zong [a], Hongwen Hu [a], Yixiang Cheng [a,*]

[a] *Key Lab of Mesoscopic Chemistry of MOE, School of Chemistry and Chemical Engineering, Nanjing University, Nanjing 210093, China*
[b] *College of Chemistry and Materials Engineering, Wenzhou University, Wenzhou 325027, China*

ARTICLE INFO

Article history:
Received 16 January 2009
Received in revised form
24 March 2009
Accepted 22 April 2009
Available online 3 May 2009

Keywords:
Chiral helical polymer
2,2′-Bipyridine
Fluorescence chemosensor

ABSTRACT

The chiral polymer **P-1** was synthesized by the polymerization of (*R*)-6,6′-dibutyl-3,3′-diiodo-2,2′-bisoctoxy-1,1′-binaphthyl (***R*-M-1**) with 5,5′-divinyl-2,2′-bipyridine (**M-1)** *via* Pd-catalyzed Heck reaction. **P-2** and **P-2′** were prepared by Wittig–Horner reaction of (*R*)-6,6′-dibutyl-2,2′-bisoctoxy-1,1′-binaphthyl-3,3′-dicarbaldehyde (***R*-M-2**) with 5,5′-bis (diethylphosphonomethyl)-2,2′-bipyridine (**M-2)** in the presence of EtONa or NaH, respectively. **P-3** was synthesized by Wittig–Horner reaction of (*R*)-6,6′-di(4-trifluoromethylphenyl)-2,2′-bisoctoxy-1,1′-binaphthyl-3,3′-dicarbaldehyde (***R*-M-3**) with **M-2** using NaH as a base. The four polymers have strong blue-green fluorescence due to the extended π-electronic structure between the chiral model compounds (*R*)-6,6′-dibutyl-/di(4-trifluoromethylphenyl)-2,2′-bisoctoxy-1,1′-binaphthyl (***R*-1** or ***R*-2**) and the conjugated linker 2,2′-bipyridyl group *via* vinylene bridge. Both monomers and polymers were analyzed by NMR, MS, FT-IR, UV–vis spectroscopy, DSC–TGA, fluorescence spectroscopy, GPC and circular dichroism (CD) spectroscopy. Based on the great differences of specific rotation values and CD spectra, **P-1** and **P-2** may adopt a zigzag chain configuration, while **P-2′** and **P-3** may adopt a helical configuration. The responsive optical properties of the two chiral helical polymers **P-2′** and **P-3** on transition metal ions were investigated by fluorescence, UV–vis and CD spectra. The results show that Ag^+ and Ni^{2+} lead to nearly complete fluorescence quenching of **P-2′** and **P-3**, Cu^{2+} and Fe^{2+} can cause obvious fluorescence quenching, but Zn^{2+} and Cd^{2+} can only produce slight fluorescence quenching. Ag^+, Ni^{2+}, Cu^{2+} and Fe^{2+} can also lead to the obvious changes of UV–vis spectra of **P-2′** and **P-3**. On the contrary, Zn^{2+} and Cd^{2+} cause little changes. Most importantly, the CD intensities and wavelengths of the chiral helical polymers **P-2′** and **P-3** exhibit the pronounced changes upon addition of Ag^+ and Ni^{2+}.

1. Introduction

Conjugated polymers based on π-conjugated organic molecules and chain backbone structures have attracted much interest during the past decade [1–6]. These functional polymers with tunable optical and electronic properties can be achieved by the careful combination of the designed monomers. They can also be used to prepare organic light-emitting diodes, electroluminescent devices, nonlinear optical materials, supramolecular sensors and other devices with colors ranging from blue to red [7–14]. Optically active 2,2′-binaphthol (BINOL) and its derivatives are one of the most important C_2 symmetric compounds and have often been used as the starting materials for the preparation of conjugated polymers that have a main-chain chiral configuration. Especially the conjugated polymer incorporating optically active binaphthyl moiety in the main-chain backbone could exhibit a sort of excellent fluorescent materials with good fluorescence quantum efficiency due to the extended π-electronic structure between the chiral repeating unit and the conjugated linker unit. These rigid and regular chiral binaphthyl-based polymers could lead to the properties of fluorescence sensors for sensitive detection of metal ions or chiral molecules recognition [15–20], asymmetric catalysts [21–26], and optoelectronic materials [27–33] by controlling the chiral organic groups and linker structure at the well-defined molecular level.

Chiral polymers with helical chain backbone have received increasing attention due to their helicity generating from secondary interactions such as hydrogen bonds and van der Waals forces. These chiral helical polymers undergo conformational change as well as helical reversal easily. But the inherently stable helical polymers are less common so far [34–36]. Takeishi and his co-workers reported that the main chains composed of rigid segments

---

* Corresponding author.
E-mail address: yxcheng@nju.edu.cn (Y. Cheng).

0032-3861/$ – see front matter © 2009 Elsevier Ltd. All rights reserved.
doi:10.1016/j.polymer.2009.04.043

are twisted to one-direction by the chiral binaphthyl linker and an ordered structure of the main-chain backbone incorporating optically pure binaphthyl could adopt the stable helical configuration [37]. As a result, there were reports on the application of some chiral helical polymers based on polybinaphthyls for electroluminescent, nonlinear optical properties and chiral sensing [21,38,39]. In view of these reports, design and synthesis of chiral helical polymers based on optically active 1,1′-binaphthyl moiety are still attractive. According to our previous report on the synthesis of polybinaphthyls, we found that a major-groove zigzag polymer and a minor-groove hexical polymer were generated while the isoquinoline moieties were introduced into the main-chain backbone by Sonogashira reaction at 6,6′- and 3,3′-postions of 1,1′-binaphthyl, respectively [40]. In this paper, we report the synthesis of four chiral polybinaphthyls incorporating 2,2′-bipyridyl moieties in the polymer main-chain backbone by Pd-catalyzed Heck reaction or Wittig–Horner reaction. As a consequence, this allows the investigation on the influence of the synthetic procedure on the chiral polymer's structure and configuration. The results indicate that **P-1** and **P-2** obtained by Heck and Wittig–Horner reaction in the presence of EtONa may adopt a zigzag form, but both **P-2**′ and **P-3** synthesized by Wittig–Horner reaction using NaH as a base may exist in a helical configuration. The responsive optical properties of two chiral helical polymers **P-2**′ and **P-3** on transition metal ions were investigated by fluorescence, UV–vis and circular dichroism (CD) spectra. The results show that **P-2**′ and **P-3** can show distinguished sensitive sense of some transition metal ions, such as Ag^+, Ni^{2+}, Cu^{2+}, Fe^{2+}, Zn^{2+} and Cd^{2+}. Such distinct ion-responsive behaviors reveal the large differences of coordination abilities of transition metal ions with 2,2′-bipyridyl ligand receptors in the helical polymer main-chain backbone. The results also suggest that 2,2′-bipyridyl moiety can act as the recognition site of a special chemosensor for sensitive detection of transition metal ions.

2. Experimental part

2.1. Materials

All solvents and reagents were commercially available and analytical-reagent-grade. (*R*)-1,1′-Binaphthol, 3-methylpyridine and 4-trifluoromethylphenylboronic acid were purchased from Aldrich and directly used without purification. THF and Et_3N were purified by distillation from sodium in the presence of benzophenone. CCl_4 and CH_3CN were distilled from P_2O_5. 5,5′-Divinyl-2,2′-bipyridine (**M-1**) was synthesized from 3-methylpyridine by a four-step reaction according to reported literatures and needed to be kept in the dark at −4 °C before using (Scheme 1) [18,41]. (*R*)-6,6′-Dibromo-2,2′-bis(methoxymethoxy)-1,1′-binaphthyl (**1**) [42], (*R*)-6,6′-dibutyl-2,2′-binaphthol (**3**) and (*R*)-6,6′-di(4-trifluoromethylphenyl)-2,2′-binaphthol (**7**) [43] were prepared for the synthesis of monomers and chiral model compound according to reported literatures (Scheme 2).

2.2. Measurements

NMR spectra were obtained using a 300-Bruker spectrometer 300 MHz for ^1H NMR and 75 MHz for ^{13}C NMR and reported as parts per million (ppm) from the internal standard TMS. FT-IR spectra were taken on a Nexus 870 FT-IR spectrometer. UV–vis spectra were obtained from a Perkin–Elmer Lambda 25 spectrometer. Fluorescent spectra were obtained from a 48000 DSCF spectrometer. DSC–TGA was performed on a Perkin–Elmer Pyris-1 instrument under N_2 atmosphere. CD spectrum was determined with a Jasco J-810 spectropolarimeter. Specific rotation was determined with a Ruololph Research Analytical Autopol I. MS was determined on a Micromass GCT. C, H, and N of elemental analyses were performed on an Elementar Vario MICRO analyzer. Molecular weight was determined by GPC with Waters-244 HPLC pump and THF was used as solvent and relative to polystyrene standards.

2.3. Preparation of *M-2* (Scheme 1)

Compound **M-2** was prepared according to a reported method [44,45]. A mixture of 5,5′-bis(bromo methyl)-2,2′-bipyridine [41] (0.93 g, 2.72 mmol) and triethylphosphite (1.94 g, 12.76 mmol) was refluxed for 4 h. After removal of the excess triethylphosphite under reduced pressure, the residue was recrystallized from the mixture of $CHCl_3$ and *n*-hexane (1:10, v/v) to afford a white solid 5,5′-bis(diethylphosphonomethyl)-2,2′-bipyridine (**M-2**) in 80.5% yield. Mp: 107–109 °C. ^1H NMR (300 MHz, $CDCl_3$): δ 8.59 (t, 2H, $J = 1.8$ Hz), 8.37 (d, 2H, $J = 8.4$ Hz), 7.84–7.80 (m, 2H), 4.14–4.04 (m, 8H), 3.25 (s, 2H), 3.18 (s, 2H), 1.29 (t, 12H, $J = 7.2$ Hz).

2.4. Preparation of model compound *R-1* (Scheme 2)

A mixture of (*R*)-6,6′-dibutyl-2,2′-binaphthol (**3**) (0.98 g, 2.46 mmol), K_2CO_3 (2.38 g, 17.23 mmol), and n-$C_8H_{17}Br$ (1.90 g, 9.84 mmol) was dissolved in 20 mL of anhydrous CH_3CN. The solution was refluxed overnight. After being evaporated to dryness, the residue was extracted with ethyl acetate (2 × 30 mL). The solution was washed with water and brine twice and then dried over anhydrous Na_2SO_4. After removal of the solvent, the cruder product was purified by chromatography on silica gel with petroleum ether/ethyl acetate (50:1, v/v) as an eluent to afford a yellow liquid (*R*)-6,6′-dibutyl-2,2′-bisoctoxy-1,1′-binaphthyl (***R*-1**) in 83.0% yield (1.27 g). $[\alpha]_D^{25} = -20.4$ (c 0.54, THF). ^1H NMR (300 MHz, $CDCl_3$): δ 7.88 (d, 2H, $J = 8.4$ Hz), 7.66 (s, 2H), 7.15 (d, 2H, $J = 8.4$ Hz), 7.10 (dd, 2H, $J = 9.0$ Hz, 1.5 Hz), 4.00–3.90 (m, 4H), 2.76 (t, 4H,

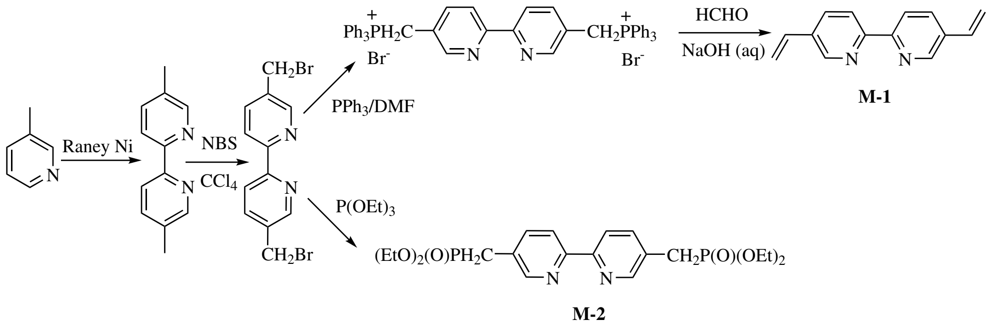

Scheme 1. Synthesis procedures of **M-1** and **M-2**.

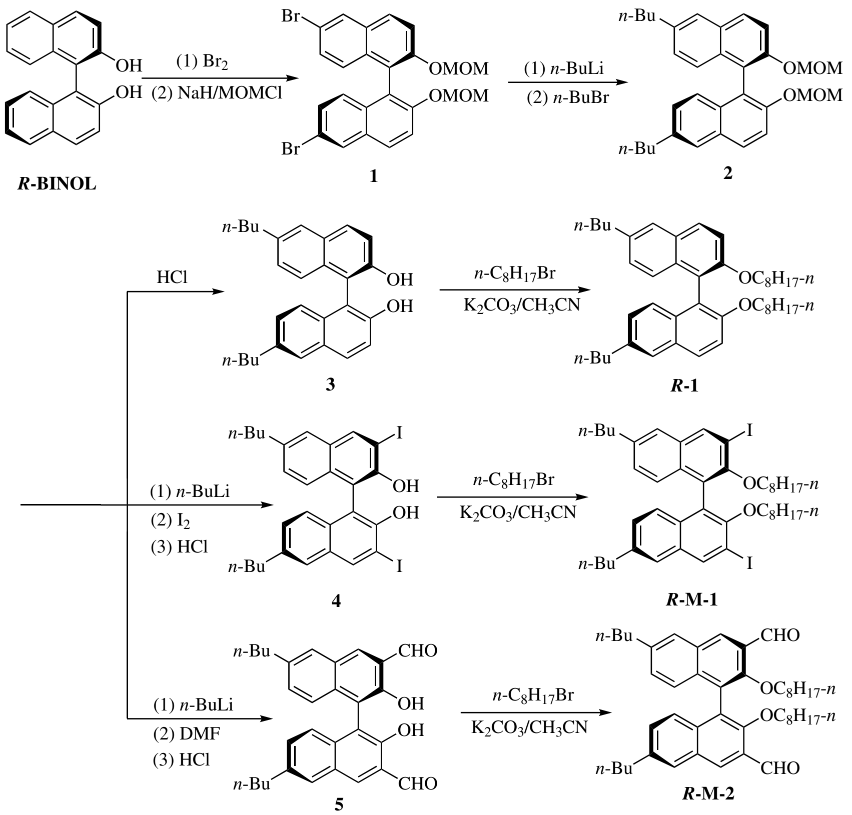

Scheme 2. Synthesis procedures of ***R*-1**, ***R*-M-1** and ***R*-M-2**.

$J = 7.5$ Hz), 1.76–1.66 (m, 4H), 1.50–1.37 (m, 9H), 1.32–1.20 (m, 4H), 1.18–0.89 (m, 31H); ^{13}C NMR (75 MHz, $CDCl_3$): δ 154.0, 137.8, 132.7, 129.5, 128.4, 127.7, 126.1, 125.6, 121.1, 116.2, 70.1, 35.6, 33.5, 31.8, 29.5, 29.2, 25.7, 22.7, 22.5, 14.2, 14.0. FT-IR (KBr, cm^{-1}): 2955, 2929, 2857, 1596, 1466, 1272, 1245, 1093. MS (EI, *m*/*z*): 622 (M^+, 100%), 510 (19%), 398 (52%), 355 (51%). Anal. Calcd for $C_{44}H_{62}O_2$: C, 84.83; H, 10.03. Found: C, 84.87; H, 10.11.

2.5. Preparation of ***R-M-1*** (Scheme 2)

(*R*)-6,6′-Dibromo-2,2′-bis(methoxymethoxy)-1,1′-binaphthyl (**1**) (5.9 g, 11.1 mmol) was dissolved in anhydrous THF (50 mL), *n*-BuLi (15.0 mL, 2.5 mol L^{-1} in hexanes, 37.5 mmol) was added by syringe injection at −78 °C under N_2 atmosphere. After the reaction mixture was stirred for 10 min, *n*-C_4H_9Br (5.3 g, 38.7 mmol) was added to the above solution at −78 °C under N_2 atmosphere. The reaction mixture was gradually warmed to room temperature and stirred overnight. The mixture was extracted with ethyl acetate (2 × 100 mL). The combined organic layers were washed with water and brine, and then dried over anhydrous Na_2SO_4. After removal of solvent under reduced pressure, the crude product was purified by column chromatography (petroleum ether/ethyl acetate) (30:1, v/v) to afford a colorless viscous product (*R*)-6,6′-dibutyl-2,2′-bis(methoxymethoxy)-1,1′-binaphthyl (**2**) in 70.4% yield (3.8 g). $[\alpha]_D^{25} = +38.0$ (*c* 0.5, CH_2Cl_2). ^{1}H NMR (300 MHz, $CDCl_3$): δ 7.93 (d, 2H, $J = 9.0$ Hz), 7.71 (s, 2H), 7.60 (d, 2H, $J = 9.0$ Hz), 7.19 (s, 4H), 5.12 (d, 2H, $J = 6.6$ Hz), 5.01 (d, 2H, $J = 6.6$ Hz), 3.21 (s, 6H), 2.79 (t, 4H, $J = 7.2$ Hz), 1.75–1.67 (m, 4H), 1.48–1.41 (m, 4H), 0.98 (t, 6H, $J = 7.2$ Hz); ^{13}C NMR (75 MHz, $CDCl_3$): δ 152.6, 138.5, 132.9, 130.4, 129.0, 128.1, 126.6, 125.9, 121.7, 117.5, 95.3, 55.7, 35.9, 33.8, 22.8, 14.3. FT-IR (KBr, cm^{-1}): 2956, 2929, 2857, 1596, 1500, 1480, 1241, 1151, 1028. MS (EI, *m*/*z*): 486 (M^+, 7%), 410 (100%), 382 (48%), 339 (34%).

Compound **2** (3.69 g, 7.58 mmol) was dissolved in 30 mL of anhydrous THF, 10.6 mL of *n*-BuLi (2.5 mol L^{-1} in hexane, 26.53 mmol) was added by syringe injection at room temperature under N_2 atmosphere. The solution was stirred for 6 h at room temperature, and then the solution of iodine (7.7 g, 30.32 mmol in 30 mL of THF) was slowly injected to the mixed solution at −78 °C under N_2 atmosphere. The mixture was then stirred overnight while the temperature was gradually warmed to room temperature. The reaction was quenched with 10% aqueous $Na_2S_2O_3$ (30 mL). After removal of the solvent under reduced pressure, the residue was extracted with ethyl acetate (2 × 50 mL), the combined organic layers were washed with water and brine twice. The solution was concentrated to give a crude product of (*R*)-6,6′-dibutyl-3,3′-diiodo-2,2′-bismethoxymethoxy-1,1′-binaphthyl which was directly used without purification. The crude product was dissolved in the mixed solvents of 30 mL of ether and 30 mL of methanol. 35 mL of HCl (12 mol L^{-1}) solution was added to the above the solution. The solution was stirred at room temperature for 8 h. After the removal of the solvent under reduced pressure, the residue was extracted with ethyl acetate (2 × 50 mL). The combined organic layers were washed with 10% aqueous Na_2CO_3 and brine twice and dried over anhydrous Na_2SO_4. After removal of solvent, a yellow viscous product (*R*)-6,6′-dibutyl-3,3′-diiodo-2,2′-binaphthol (**4**) was obtained in the yield of 38.8% (1.91 g). $[\alpha]_D^{25} = +65.0$ (*c* 0.3, CH_2Cl_2). Mp: 58–60 °C. ^{1}H NMR (300 MHz, $CDCl_3$): δ 8.47 (s, 2H), 7.58 (s, 2H), 7.19 (dd, 2H, $J = 8.7$ Hz, 1.5 Hz), 7.03 (d, 2H, $J = 8.7$ Hz), 5.36 (s, 2H), 2.74 (t, 4H, $J = 7.5$ Hz), 1.69–1.61 (m, 4H), 1.43–1.36 (m, 4H), 0.99–0.90 (m, 6H); ^{13}C NMR (75 MHz, $CDCl_3$): δ 149.5, 139.7, 139.3, 131.5, 130.8, 129.5, 125.6, 124.3, 112.5, 86.3, 35.4, 33.3, 22.3, 13.9. FT-IR (KBr, cm^{-1}): 3476, 2925, 2854, 1572, 1500, 1441, 1362, 1143. MS (EI, *m*/*z*): 650 (M^+, 100%), 607 (100%).

A mixture of compound **4** (1.7 g, 2.62 mmol), K_2CO_3 (2.53 g, 18.34 mmol), and *n*-$C_8H_{17}Br$ (2.0 g, 10.46 mmol) was dissolved in

80 mL of anhydrous CH_3CN. The solution was refluxed overnight. After being evaporated to dryness, the residue was extracted with ethyl acetate (2 × 50 mL). The solution was washed with water and brine twice and then dried over anhydrous Na_2SO_4. After removal of solvent, the crude product was purified by chromatography on silica gel with petroleum ether/ethyl acetate (40:1, v/v) as an eluent to afford a yellow liquid (*R*)-6,6′-dibutyl-3,3′-diiodo-2,2′-bisoctoxy-1,1′-binaphthyl (***R*-M-1**) in 77.8% yield (1.78 g). $[\alpha]_D^{25} = -17.9$ (*c* 0.73, THF). ^1H NMR (300 MHz, $CDCl_3$): δ 8.43 (s, 2H), 7.54 (s, 2H), 7.13 (dd, 2H, *J* = 8.7 Hz, 1.8 Hz), 7.06 (d, 2H, *J* = 8.7 Hz), 3.86–3.79 (m, 2H), 3.38–3.31 (m, 2H), 2.74 (t, 4H, *J* = 7.8 Hz), 1.72–1.62 (m, 4H), 1.43–1.33 (m, 4H), 1.30–1.21 (m, 9H), 1.17–1.03 (m, 7H), 0.98–0.88 (m, 16H), 0.85–0.82 (m, 4H); ^{13}C NMR (75 MHz, $CDCl_3$): δ 153.3, 139.7, 138.8, 132.3, 132.2, 128.3, 125.8, 125.6, 125.0, 92.9, 73.3, 35.4, 33.1, 31.7, 29.6, 29.1, 28.9, 25.3, 22.6, 22.3, 14.1, 13.9. FT-IR (KBr, cm^{-1}): 2954, 2927, 2856, 1568, 1465, 1228, 1149, 1026. MS (EI, *m*/*z*): 874 (M^+, 2%), 762 (5%), 650 (100%), 607 (4%). Anal. Calcd for $C_{44}H_{60}I_2O_2$: C, 60.41; H, 6.91. Found: C, 60.47; H, 6.86.

2.6. Preparation of ***R*-M-2** (Scheme 2)

Compound **2** (3.36 g, 6.6 mmol) was dissolved in anhydrous THF (80 mL), *n*-BuLi (9.4 mL, 2.5 mol L^{-1} in hexanes, 23.5 mmol) was added by syringe injection at room temperature under a N_2 atmosphere. The mixture was first stirred for 2 h, and then cooled to 0 °C. 1.9 mL of DMF (24.8 mmol) was added to the above solution. The reaction mixture was gradually warmed to room temperature and continued to stir for 4 h. After 60 mL of HCl (12 mol L^{-1}) was added to the solution, the solution was stirred at room temperature overnight. After the removal of the solvent under reduced pressure, the residue was extracted with CH_2Cl_2 (3 × 50 mL). The combined extract was washed with 100 mL of saturated $NaHCO_3$ solution and brine twice and then dried over anhydrous Na_2SO_4. After removal of solvent under reduced pressure, the crude product was purified by column chromatography (petroleum ether/ethyl acetate) (10:1, v/v) to afford (*R*)-6,6′-dibutyl-3,3′-diformyl-2,2′-binaphthol (**5**) as yellow solids in 38.4% yield (1.2 g). $[\alpha]_D^{25} = +216.0$ (*c* 0.5, CH_2Cl_2). Mp: 150–152 °C. ^1H NMR (300 MHz, $CDCl_3$): δ 10.55 (s, 2H), 10.19 (s, 2H), 8.28 (s, 2H), 7.77 (s, 2H), 7.30 (dd, 2H, *J* = 8.7, 1.8 Hz), 7.15 (d, 2H, *J* = 8.7 Hz), 2.75 (t, 4H, *J* = 7.8 Hz), 1.73–1.67 (m, 4H), 1.47–1.35 (m, 4H), 0.96 (t, 6H, *J* = 7.2 Hz); ^{13}C NMR (75 MHz, $CDCl_3$): δ 196.9, 153.1, 139.0, 137.9, 136.0, 132.5, 128.2, 127.9, 124.8, 122.1, 116.6, 35.3, 33.2, 22.4, 14.0. FT-IR (KBr, cm^{-1}): 3426, 2955, 2928, 2856, 1658, 1506, 1377, 1294. MS (EI, *m*/*z*): 454 (M^+, 100%), 436 (11%), 411 (21%), 393 (15%). Anal. Calcd for $C_{30}H_{30}O_4$: C, 79.27; H, 6.65. Found: C, 79.21; H, 6.67.

By using the same procedure as for the preparation of ***R*-M-1**, (*R*)-6,6′-dibutyl-2,2′-bisoctoxy-1,1′-binaphthyl-3,3′-dicarbaldehyde (***R*-M-2**) was obtained as a yellow liquid in 76.4% yield from compound **5**. $[\alpha]_D^{25} = -17.7$ (*c* 0.62, THF). ^1H NMR (300 MHz, $CDCl_3$): δ 10.57 (s, 2H), 8.53(s, 2H), 7.82 (s, 2H), 7.27 (dd, 2H, *J* = 9.0, 1.8 Hz), 7.15 (d, 2H, *J* = 8.7 Hz), 3.81–3.74 (m, 2H), 3.50–3.42 (m, 2H), 2.77 (t, 4H, *J* = 7.5 Hz), 1.74–1.64 (m, 4H), 1.47–1.34 (m, 4H), 1.30–1.16 (m, 9H), 1.11–1.01 (m, 4H), 0.96 (t, 9H, *J* = 7.2 Hz), 0.86 (t, 9H, *J* = 7.2 Hz), 0.81–0.74 (m, 5H); ^{13}C NMR (75 MHz, $CDCl_3$): δ 190.2, 155.7, 140.3, 135.6, 131.0, 130.9, 130.1, 128.9, 128.6, 125.7, 125.4, 76.3, 35.4, 33.2, 31.7, 29.7, 29.0, 28.9, 25.4, 22.6, 22.4, 14.1, 13.9. FT-IR (KBr, cm^{-1}): 2927, 2856, 1693, 1591, 1325, 1127, 1071. MS (EI, *m*/*z*): 678 (M^+, 10%), 566 (34%), 451 (100%), 436 (17%). Anal. Calcd for $C_{46}H_{62}O_4$: C, 81.37; H, 9.20. Found: C, 81.39; H, 9.14.

2.7. Preparation of model compound ***R*-2** (Scheme 3)

By using the same procedure as for the preparation of ***R*-1**, (*R*)-6,6′-di(4-trifluoromethylphenyl)-2,2′-bisoctoxy-1,1′-binaphthyl (***R*-2**) was obtained as a yellow solid in 79.5% yield from compound **7**. $[\alpha]_D^{25} = -69.9$ (*c* 0.54, THF). Mp: 78–81 °C. ^1H NMR (300 MHz, $CDCl_3$): δ 8.12 (d, 2H, *J* = 1.8 Hz), 8.05 (d, 2H, *J* = 9.0 Hz), 7.80 (d, 4H, *J* = 8.1 Hz), 7.72 (d, 4H, *J* = 8.4 Hz), 7.50 (dd, 2H, *J* = 8.7, 2.7 Hz), 7.31 (d, 2H, *J* = 8.7 Hz), 4.06–3.97 (m, 4H), 1.48–1.41 (m, 4H), 1.23–0.95 (m, 20H), 0.8 (t, 6H, *J* = 7.2 Hz); ^{13}C NMR (75 MHz, $CDCl_3$): δ 155.2, 144.8, 134.5, 133.9, 129.8, 129.3, 128.8, 127.4, 126.4, 126.3, 125.7, 125.5, 122.6, 120.2, 116.3, 69.7, 31.8, 29.4, 29.2, 29.1, 25.8, 22.6, 14.0. FT-IR (KBr, cm^{-1}): 2926, 2815, 1615, 1591, 1468, 1325, 1247, 1113, 1071. MS (EI) *m*/*z* = 798 (M^+, 91%), 686 (8%), 574 (100%). Anal. Calcd for $C_{30}H_{30}O_4$: C, 75.17; H, 6.56. Found: C, 75.27; H, 6.65.

2.8. Preparation of ***R*-M-3** (Scheme 3)

Compound **1** (1.5 g, 2.82 mmol), 4-trifluoromethylphenylboronic acid (1.88 g, 9.86 mmol) and $Pd(PPh_3)_4$ (326 mg, 0.28 mmol) were mixed in DME (30 mL) under N_2 atmosphere. 2 mol L^{-1} K_2CO_3 solution (7.4 mL) was added to the above the solution. The resulting mixture was stirred and refluxed for 10 h under N_2 atmosphere. The mixture was cooled to room temperature, and the solution was filtered through a short column of silica gel with ethyl acetate as an eluent. After removal of solvents under reduced pressure, the residue was extracted by ethyl acetate (2 × 30 mL) and washed with

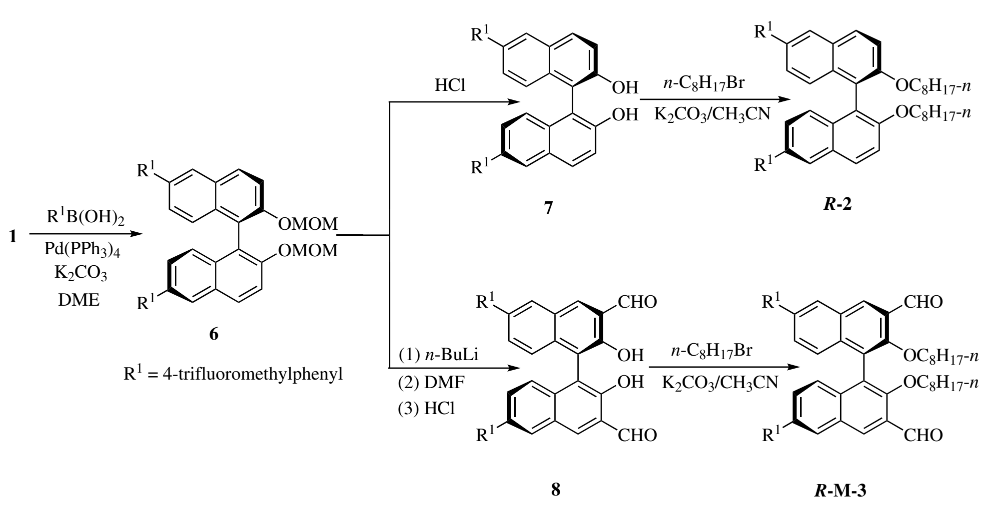

Scheme 3. Synthesis procedures of ***R*-2** and ***R*-M-3**.

water and brine twice and dried over anhydrous Na_2SO_4. After removal of solvents, the crude product was purified on silica column using the mixed solvents of petroleum ether and ethyl acetate (20:1, v/v) as an eluent to afford a white solid (*R*)-6,6′-di(4-trifluoromethylphenyl)-2,2′-bis(methoxymethoxy)-1,1′-binaphthyl (**6**) in 85.6% yield (1.60 g). $[\alpha]_D^{25} = -88.0$ (*c* 0.5, CH_2Cl_2). Mp: 84–86 °C. ^1H NMR (300 MHz, $CDCl_3$): δ 8.15 (d, 2H, *J* = 1.5 Hz), 8.08 (d, 2H, *J* = 9.0 Hz), 7.82–7.68 (m, 10H), 7.53 (dd, 2H, *J* = 9.0, 1.8 Hz), 7.31 (d, 2H, *J* = 9.0 Hz), 5.16 (d, 2H, *J* = 6.9 Hz), 5.07 (d, 2H, *J* = 6.9 Hz), 3.23 (s, 6H); ^{13}C NMR (75 MHz, $CDCl_3$): δ 153.3, 144.5, 135.3, 133.7, 130.1, 130.0, 127.5, 126.5, 126.4, 125.9, 125.8, 125.7, 120.9, 117.9, 95.15, 56.0. FT-IR (KBr, cm^{-1}): 2957, 2903, 1616, 1596, 1496, 1325, 1123, 1069. MS (EI, *m*/*z*): 662 (M^+, 4%), 586 (100%), 558 (94%).

Compound **6** (1.40 g, 2.11 mmol) was dissolved in anhydrous THF (40 mL), *n*-BuLi (2.95 mL, 2.5 mol L^{-1} in hexane, 7.39 mmol) was added by syringe injection at room temperature under N_2 atmosphere. The mixture was first stirred for 2 h, and then cooled to 0 °C. 0.59 mL of DMF (7.64 mmol) was added to the above solution. The reaction mixture was gradually warmed to room temperature and continued to stir for 4 h. After 20 mL of HCl (12 mol L^{-1}) was added to the solution, the solution was stirred at room temperature overnight. After the removal of the solvent under reduced pressure, the residue was extracted with CH_2Cl_2 (3 × 20 mL). The combined extract was washed with 60 mL of saturated $NaHCO_3$ solution and brine twice and then dried over anhydrous Na_2SO_4. After removal of the solvent under reduced pressure, the crude product was purified by column chromatography (petroleum ether/ethyl acetate) (20:1, v/v) to afford (*R*)-6,6′-di(4-trifluoromethylphenyl)-3,3′-diformyl-2,2′-binaphthol (**8**) as a yellow solid in 28.5% (0.38 g). $[\alpha]_D^{25} = +84.6$ (*c* 0.37, THF). Mp: 252–254 °C. ^1H NMR (300 MHz, $CDCl_3$): δ 10.73 (s, 2H), 10.26 (s, 2H), 8.47 (s, 2H), 8.24 (s, 2H), 7.78–7.70 (m, 10H), 7.38 (d, 2H, *J* = 8.7 Hz); ^{13}C NMR (75 MHz, $CDCl_3$) δ: 196.8, 154.3, 143.7, 138.9, 136.9, 135.9, 130.1, 128.2, 127.8, 127.4, 126.0, 125.9, 125.7, 122.7, 122.4, 116.4. FT-IR (KBr, cm^{-1}): 3444, 3078, 2928, 2844, 2735, 1662, 1616, 1503, 1327, 1136, 1071. MS (EI, *m*/*z*): 630 (M^+, 100%), 612 (42%). Anal. Calcd for $C_{30}H_{30}O_4$: C, 68.57; H, 3.20. Found: C, 68.77; H, 3.25.

By using the same procedure as for the preparation of ***R*-M-2**, (*R*)-6,6′-bis(4-trifluoromethylphenyl)-2,2′-bisoctoxy-1,1′-binaphthyl-3,3′-dicarbaldehyde (***R*-M-3**) was obtained as a yellow liquid in 41.2% yield from compound **8**. $[\alpha]_D^{25} = -56.4$ (*c* 0.5, THF). ^1H NMR (300 MHz, $CDCl_3$): δ 10.62 (s, 2H), 8.72 (s, 2H), 8.32 (d, 2H, *J* = 1.8 Hz), 7.80 (q, 8H, *J* = 9.0 Hz), 7.71 (dd, 2H, *J* = 7.8, 1.8 Hz), 7.39 (d, 2H, *J* = 8.7 Hz), 3.89–3.82 (m, 2H), 3.61–3.54 (m, 2H), 1.36–1.28 (m, 6H), 1.15–1.13 (m, 4H), 1.09–0.94 (m, 8H), 0.90–0.79 (m, 12H); ^{13}C NMR (75 MHz, $CDCl_3$): δ 190.2, 156.8, 143.4, 137.2, 136.5, 132.1, 130.1, 129.6, 128.8, 128.6, 127.5, 126.6, 126.0, 125.9, 125.3, 122.4, 76.6, 31.7, 29.8, 29.1, 29.0, 25.6, 22.6, 14.0. FT-IR (KBr, cm^{-1}): 2956, 2928, 2857, 1692, 1590, 1446, 1115. MS (EI, *m*/*z*): 854 (M^+, 3%), 742 (12%), 630 (100%), 612 (39%). Anal. Calcd for $C_{52}H_{52}F_6O_4$: C, 73.05; H, 6.13. Found: C, 73.15; H, 6.09.

2.9. Preparation of *P-1*, *P-2*, *P-2′* and *P-3* (Scheme 4)

A mixture of ***R*-M-1** (139.9 mg, 0.16 mmol) and **M-1** (34.8 mg, 0.16 mmol) was dissolved in the mixed solvents of 6 mL DMF and

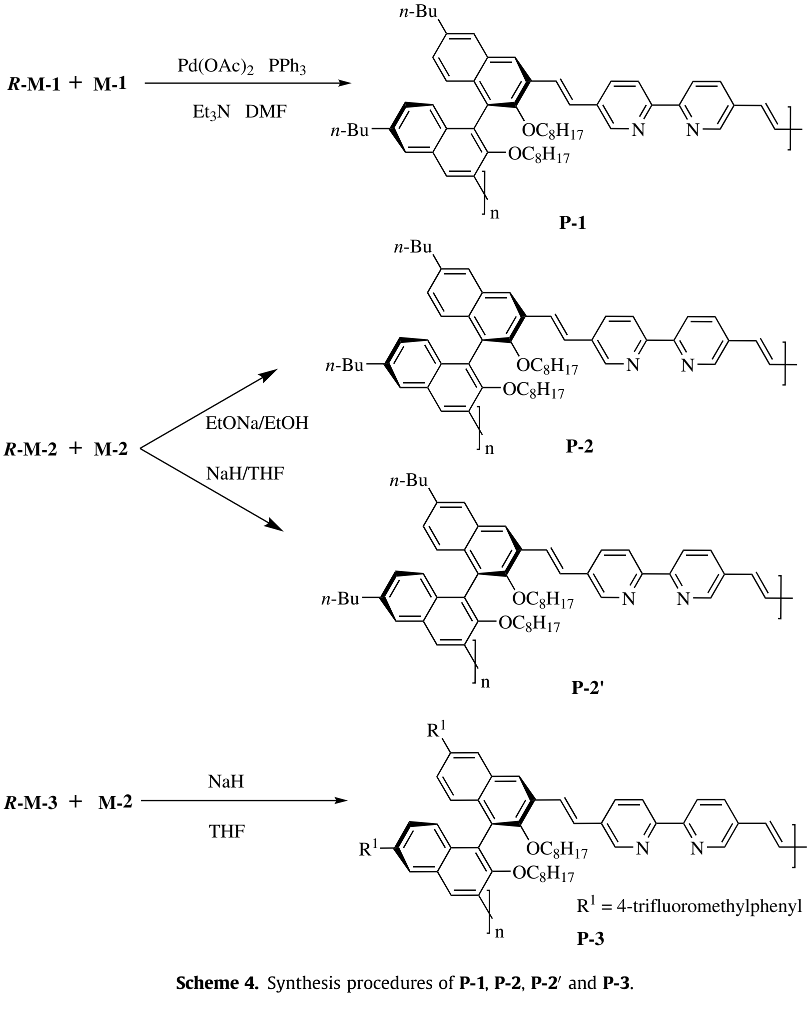

Scheme 4. Synthesis procedures of **P-1**, **P-2**, **P-2′** and **P-3**.

0.2 mL Et_3N. The solution was first bubbled with N_2 for 15 min before 5 mol% $Pd(OAc)_2$ (1.9 mg, 0.0084 mmol) and 25 mol% PPh_3 (11.0 mg, 0.042 mmol) were added to the above solution. The temperature of the mixture was kept at 120 °C for 12 h under N_2, and then refluxed at 130 °C for an additional 2 h. The mixture was cooled to room temperature, and then was filtered through a short silica gel column in methanol (50 mL) to precipitate out the polymer. The resulting polymer was filtered and washed with methanol several times. Further purification could be conducted by dissolving the polymer in THF to precipitate in methanol again. **P-1** was dried in vacuum to give 56.2 mg in 42.5% yield. **P-1** spectroscopic data: $[\alpha]_D^{25} = -236.8$ (c 0.05, THF); ^{1}H NMR (300 Hz, $CDCl_3$): δ 8.88 (br, 2H), 8.49–8.45 (m, 2H), 8.23 (br, 2H), 8.06–8.04 (m, 2H), 7.82–7.81 (m, 2H), 7.72 (br, 2H), 7.46–7.41 (m, 2H), 7.18–7.11 (m, 4H), 3.79–3.76 (m, 2H), 3.39–3.37 (m, 2H), 2.79–2.73 (m, 4H), 1.76–1.65 (m, 8H), 1.45–1.35 (m, 6H), 1.21-0.77 (m, 30H). FT-IR (KBr, cm^{-1}): 3042, 2924, 2853, 1589, 1465, 1228, 1120. Anal. Calcd for $C_{58}H_{70}N_2O_2$: C, 84.22; H, 8.53; N, 3.39. Found: C, 81.42; H, 8.39; N, 3.45.

A mixture of ***R*-M-2** (149.4 mg, 0.22 mmol) and **M-2** (100.3 mg, 0.22 mmol) and EtONa (50.3 mg, 0.74 mmol) was dissolved in absolute anhydrous EtOH (20 mL). The solution was refluxed for 18 h under N_2 atmosphere. After being evaporated to dryness, the residue was extracted with CH_2Cl_2 (3 × 50 mL). The solution was washed with water and then dried over anhydrous Na_2SO_4. After the solvent was removed under reduced pressure, the residue was dissolved by a small quantity of THF, and 60 mL of methanol was added to precipitate the polymer. A yellow solid was filtered off and washed with methanol several times. Further purification could be conducted by dissolving the polymer in CH_2Cl_2 to precipitate in methanol again. The polymer was dried under vacuum at room temperature for 24 h. The final yield was 84.2% (153.2 mg). **P-2** spectroscopic data: $[\alpha]_D^{25} = -158.3$ (c 0.05, THF); ^{1}H NMR (300 Hz, $CDCl_3$): δ 8.88 (br, 2H), 8.49–8.46 (m, 2H), 8.24 (br, 2H), 8.08–8.03 (m, 2H), 7.80–7.79 (m, 2H), 7.72 (br, 2H), 7.46–7.39 (m, 2H), 7.18–7.09 (m, 4H), 3.79–3.73 (m, 2H), 3.39–3.35 (m, 2H), 2.79–2.72 (m, 4H), 1.76–1.64 (m, 8H), 1.46–1.36 (m, 6H), 1.24–0.72 (m, 30H). FT-IR (KBr, cm^{-1}): 3041, 2924, 2853, 1589, 1466, 1227, 1120. Anal. calcd for $C_{58}H_{70}N_2O_2$: C, 84.22; H, 8.53; N, 3.39. Found: C, 81.92; H, 8.43; N, 3.29.

A mixture of ***R*-M-2** (149.4 mg, 0.22 mmol) and **M-2** (100.3 mg, 0.22 mmol) and NaH (21.1 mg, 0.88 mmol) was dissolved in anhydrous THF (20 mL). The solution was refluxed for 18 h under N_2 atmosphere. After being evaporated to dryness, the residue was extracted with CH_2Cl_2 (3 × 50 mL). The solution was washed with water and then dried over anhydrous Na_2SO_4. After the solvent was removed under reduced pressure, the residue was dissolved by a small quantity of THF, and 60 mL of methanol was added to precipitate the polymer. A yellow solid was filtered off and washed with methanol several times. Further purification could be conducted by dissolving the polymer in CH_2Cl_2 to precipitate in methanol again. The polymer was dried under vacuum at room temperature for 24 h. The final yield was 86.3% (157.0 mg). **P-2′** spectroscopic data: $[\alpha]_D^{25} = -758.4$ (c 0.025, THF); ^{1}H NMR (300 Hz, $CDCl_3$): δ 8.88 (s, 2H), 8.48 (d, 2H, J = 8.4 Hz), 8.23 (s, 2H), 8.07–8.04 (m, 2H), 7.79 (d, 2H, J = 16.5 Hz), 7.72 (s, 2H), 7.43 (d, 2H, J = 16.5 Hz), 7.20–7.10 (m, 4H), 3.78–3.75 (m, 2H), 3.41–3.37 (m, 2H), 2.77–2.75 (m, 4H), 1.78–1.59 (m, 8H), 1.48–1.36 (m, 6H), 1.23–0.80 (m, 30H). FT-IR (KBr, cm^{-1}): 3042, 2925, 2854, 1592, 1466, 1230, 1119, 966. Anal. Calcd for $C_{58}H_{70}N_2O_2$: C, 84.22; H, 8.53; N, 3.39. Found: C, 80.07; H, 8.24; N, 3.37.

By using the same procedure as for the preparation of **P-2′**, **P-3** was obtained from ***R*-M-3** and **M-2** as a yellow solid in 80.4% yield.

P-3 spectroscopic data: $[\alpha]_D^{25} = -410.6$ (c 0.025, THF). ^{1}H NMR (300 Hz, $CDCl_3$): δ 8.92 (s, 2H), 8.52–8.50 (m, 2H), 8.22 (br, 2H), 8.10–8.08 (m, 2H), 7.83–7.75 (m, 12H), 7.58–7.55 (m, 4H), 7.40–6.37 (m, 2H), 3.85–3.82 (m, 2H), 3.50–3.46 (m, 2H), 1.38–0.75 (m, 30H). FT-IR (KBr, cm^{-1}): 3044, 2925, 2854, 1616, 1590, 1466, 1325, 1125, 1070, 965. Anal. Calcd for $C_{64}H_{60}N_2O_2F_6$: C, 76.63; H, 6.03; N, 2.79. Found: C, 76.57; H, 6.07; N, 2.74.

2.10. Metal ion titration

Each metal ion titration experiment was started with a 3.0 mL polymer in THF solution with a known concentration (3.0×10^{-5} mol L^{-1}). Solutions of metal salt (acetate, nitrate and sulfate, 5.0×10^{-3} mol L^{-1}) were used for the titration. Polymer–metal complexes were produced by adding aliquots of a solution of the selected metal salt to a THF solution of the chiral polymer. The mixture was stirred constantly during the titration. All measurements were monitored 15 min after addition of the metal salt to the polymer solutions.

3. Results and discussion

3.1. Syntheses and feature of the chiral polymers

5,5′-Bis(diethylphosphonomethyl)-2,2′-bipyridine (**M-2**) was obtained by the reaction of 5,5′-bis(bromomethyl)-2,2′-bipyridine with an excess of triethylphosphite in 80.5% yield (Scheme 1) [44,45]. The synthesis procedures of (*R*)-6,6′-dibutyl-2,2′-bis(methoxymethoxy)-1,1′-binaphthyl (**2**), the chiral model compound (*R*)-6,6′-dibutyl-2,2′-bisoctoxy-1,1′-binaphthyl (***R*-1**), (*R*)-6,6′-dibutyl-3,3′-diiodo-2,2′-binaphthol (**4**), (*R*)-6,6′-dibutyl-3,3′-diiodo-2,2′-bisoctoxy-1,1′-binaphthyl (***R*-M-1**), (*R*)-6,6′-dibutyl-3,3′-diformyl-2,2′-binaphthol (**5**) and (*R*)-6,6′-dibutyl-2,2′-bisoctoxy-1,1′-binaphthyl-3,3′-dicarbaldehyde (***R*-M-2**) are shown in Scheme 2 [18,46–51]. Compound **2** was first lithiated with *n*-BuLi, and then followed by carbonylation to afford the MOM-protected intermediate, which was then hydrolysed in HCl solution to afford the crude product **5**. The purification of **5** could be carried out by column chromatography on silica gel to afford a yellow solid product in 38.4% yield. The etherification of hydroxyl groups of **5** could be carried out by reaction with *n*-octyl bromide in the presence of K_2CO_3 to afford ***R*-M-2** with a satisfactory yield. (*R*)-6,6′-Di(4-trifluoromethylphenyl)-2,2′-bis(methoxymethoxy)-1,1′-binaphthyl (**6**), the chiral model compound (*R*)-6,6′-di(4-trifluoromethylphenyl)-2,2′-bisoctoxy-1,1′-binaphthyl (***R*-2**), (***R***)-6,6′-di(4-trifluoromethylphenyl)-3,3′-diformyl-2,2′-binaphthol (**8**) and (*R*)-6,6′-di(4-trifluoromethylphenyl)-2,2′-bisoctoxy-1,1′-binaphthyl-3,3′-dicarbaldehyde (***R*-M-3**) were prepared and purified according to reported literatures (Scheme 3) [43,52–54]. Compound **8** was prepared by using the same procedure as compound **5**, but it was only obtained in 28.5% yield due to the influence of strong electron-withdrawing CF_3 group. ***R*-M-1**, ***R*-M-2** and ***R*-M-3** could be served as the chiral monomers for the synthesis of the chiral polymers **P-1**, **P-2**, **P-2′** and **P-3**.

The chiral conjugated polymers **P-1**, **P-2** and **P-2′** have the same chain backbone structure containing (*R*)-6,6′-dibutyl-2,2′-bisoctoxy-1,1′-binaphthyl and 2,2′-bipyridyl group *via* vinylene bridge. But they were prepared by different reactions or under different reaction conditions (Scheme 4). In this paper, a typical Heck reaction condition was applied to the synthesis of **P-1**, the polymerization was easily carried out by the chiral monomer ***R*-M-1** with **M-1** in the presence of a catalytic amount (5 mol%) of $Pd(OAc)_2$ with Et_3N and triphenylphosphate (PPh_3) under N_2 [18]. **P-2** and **P-2′** were synthesized by Wittig–Horner reaction of the chiral monomer ***R*-M-2** with **M-2** in the presence of EtONa or NaH, respectively [28,32,45,55]. **P-3** was synthesized by Wittig–Horner reaction of ***R*-M-3** with **M-2** by using NaH as a base. But we found that **P-3** could not be obtained in a high molecular weight if NaH was replaced by EtONa. The gel permeation chromatography (GPC) analysis and the

Table 1
Polymerization results and characterization of **P-1**, **P-2**, **P-2′** and **P-3**.

	Yield (%)	M_w[a]	M_n[a]	PDI	$[\alpha]_D$[b]
P-1	42.5	7330	3630	2.02	−236.8
P-2	84.2	8980	3280	2.74	−158.3
P-2′	86.3	11590	5900	1.96	−758.4
P-3	80.4	11400	3530	3.23	−410.6

[a] M_w, M_n and PDI of **P-1**, **P-2**, **P-2′** and **P-3** were determined by gel permeation chromatography using polystyrene standards in THF.
[b] Temperature at 25 °C and solvent in THF.

specific rotation results of the four polymers are listed in Table 1. The GPC results of the polymers **P-1**, **P-2**, **P-2′** and **P-3** show the moderate molecular weight. Furthermore we also found that the chiral polymers **P-2**, **P-2′** and **P-3** have higher molecular weights by Wittig–Horner reaction than **P-1** obtained by Heck polymerization method, which is consistent with previous reports [56,57].

The chiral conjugated polymers show good solubility in some common solvents, such as toluene, THF, $CHCl_3$, and CH_2Cl_2, which can be attributed to the nonplanarity of the twisted polymers in the main-chain backbone and the flexible octoxy, *n*-butyl or 4-trifluorophenyl group substitutents on binaphthyl units as side chain of the polymer. In this paper, we report synthesis and fluorescence property of chiral polybinaphthyls incorporating 2,2′-bipyridyl moieties in the polymer main chain. An electron-deficient ligand 2,2′-bipyridine as the conjugated bridge linker and a metal chelating ligand was introduced into the chiral polybinaphthyl's main-chain backbone to maintain conjugation between bipyridyl and naphthyl segments so that the electron transporting properties of the polymers may be improved and the electron density may shift away *via* vinylene bridge. Furthermore, the vinylene bridge can reduce steric hindrance between naphthyl and bipyridyl groups, and also has a beneficial influence on the stability of the resulting chiral polymers [9,11,41,58,59]. This chelating bipyridyl ligand can orient in a well-defined spatial arrangement in the chiral polymers main-chain and also directly coordinate with different transition metal ions to form metal–polymer complexes. All four chiral conjugated polymers have strong blue-green fluorescence. Based on fluorescent and UV–vis spectra, the results show that the chiral polymers have been found to be highly sensitive to a wide variety of metal ions, and their fluorescence is efficiently or completely quenched upon the addition of transition metal ions.

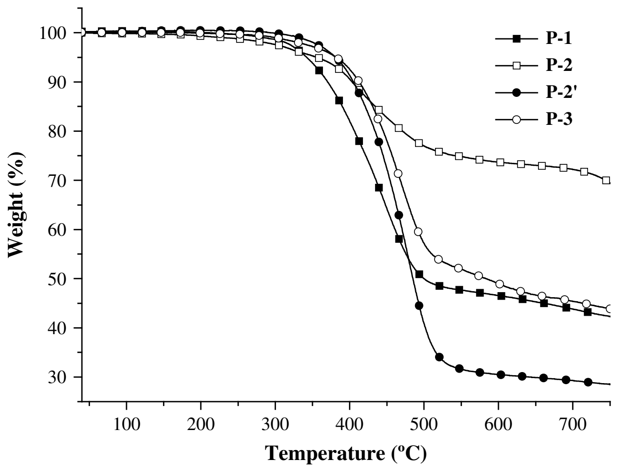

Fig. 1. TGA curves of **P-1**, **P-2**, **P-2′** and **P-3**.

Table 2
Optical properties of **P-1**, **P-2**, **P-2′** and **P-3**.

	UV–vis (λ_{max})[a]	PL (λ_{max})[a]		Stokes shift (nm)[b]	Φ_{PL}[c]
		λ_{ex}	λ_{em}		
M-1	273 (w), 321	347	364, 382 (sh)	–	–
***R*-1**	240, 344 (w)	345	364	–	–
***R*-2**	268, 307	344	377	–	–
P-1	240, 373	363	434, 455	82	0.50
P-2	238, 383	364	458	74	0.35
P-2′	236, 384	345	437, 460	76	0.43
P-3	261, 294, 384	342	437, 458	74	0.45

[a] Determined in THF solution.
[b] Stokes shift = PL λ_{max} (nm) − UV–vis λ_{max} (nm).
[c] These values were estimated by using the quinine sulfate solution (ca. 1.0×10^{-5} mol L^{-1}) in 0.5 mol L^{-1} H_2SO_4 (Φ_f = 55%) as a standard.

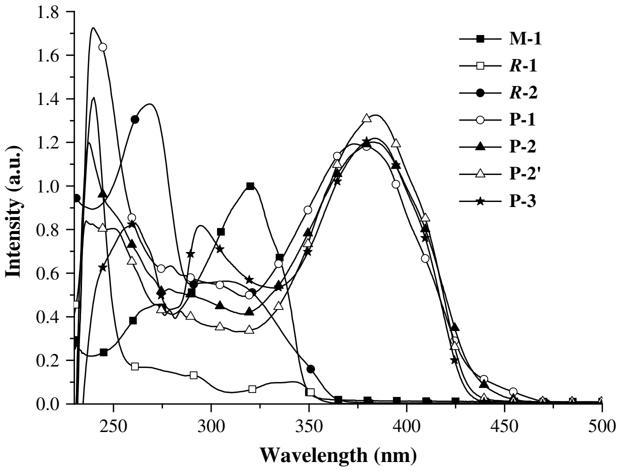

Fig. 2. UV–vis spectra of **M-1**, **R-1**, **R-2**, **P-1**, **P-2**, **P-2′** and **P-3**.

The chirality of BINOL and its derivatives is derived from the restricted rotation of the two naphthalene rings. The rigid structure and C_2 symmetry of the chiral binaphthyl molecules can play an important role in inherently chiral induction. The dihedral angle between two naphthalene rings of a binaphthyl molecule ranges from 60° to 120°, which leads to the kinked or twisted polymer main-chain backbone [21,60,61]. According to Samyn's report [30,31], the chiral polymer incorporating chiral *R* or *S* binaphthyl

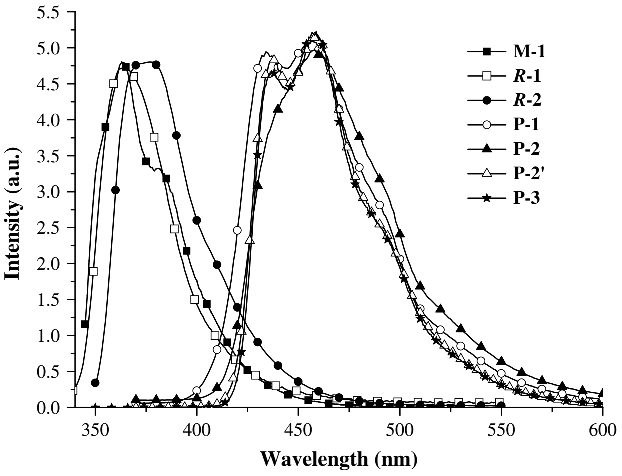

Fig. 3. Fluorescence spectra of the repeating units and **P-1**, **P-2**, **P-2′** and **P-3**.

Table 3
CD spectra data of ***R*-1** and ***R*-2**, **P-1**, **P-2**, **P-2′** and **P-3** in THF.

	***R*-1** × 10^5	***R*-2** × 10^5	**P-1** × 10^5	**P-2** × 10^5	**P-2′** × 10^5	**P-3** × 10^5
[θ] (λ_{max} in nm)	−6.91	+1.66	−1.28	−0.70	−2.59	+0.65
	(229.1)	(226.2)	(238.0)	(236.9)	(232.9)	(239.2)
	+9.54	+4.95	+0.39	+0.23	+0.88	−1.37
	(240.3)	(256.5)	(263.7)	(263.0)	(258.1)	(256.5)
	−0.42	−6.59	+0.41	+0.22	+0.78	−0.89
	(287.0)	(275.0)	(279.1)	(283.2)	(304.5)	(285.7)
			+0.35	+0.31	+1.87	+1.33
			(352.9)	(361.5)	(361.7)	(317.3)
			−0.63	−0.52	−2.97	+1.85
			(399.4)	(409.8)	(408.8)	(363.1)
						−2.71
						(407.7)

units in the main chain of polymer backbone can adopt a helical configuration. But no helical configuration can be formed if racemic 1,1′-binaphthyl monomers are incorporated into the same polymer backbone, it may form a random-coil-like structure. He pointed out that polymers are helices due to the twisted configuration of the binaphthyl moieties if chiral binaphthyl units are connected through rigid groups. A helix is highly regular structure, which all bonds have the same configuration (either *R* or *S*). Yashima thought the generation of a helical structure should result in significant chiral amplification [62]. In this paper, the specific rotation values ($[\alpha]_D^{25}$) of the chiral polymers **P-2′** and **P-3** greatly fluctuate to −758 and −411 (*c* 0.05, THF) and are much larger than those of ***R*-1**, ***R*-2**, **P-1** and **P-2**, and dramatic changes are observed in the CD spectra of these two chiral polymers compared with other compounds. It can be concluded that a helical configuration of **P-2′** and **P-3** should be generated [16,40].

3.2. Thermal analysis of polymers

P-1, **P-2**, **P-2′** and **P-3** are air stable solid with yellow-green color. Based on the results of differential scanning calorimetry (DSC), **P-1**, **P-2′** and **P-3** show no glass transition temperature (T_g), but **P-2** shows a T_g at 192 °C. Thermogravimetric analyses (TGA) of these polymers were carried out under a N_2 atmosphere at a heating rate of 10 °C/min. As show in Fig. 1, although the repeating units of **P-1**, **P-2** and **P-2′** are the same polymer composition and backbone chain structure, their TGA plots are different. Under a N_2 atmosphere, **P-1**, **P-2** and **P-2′** show an apparently one-step degradation at temperature ranging from 340 to 550 °C, 330 to 560 °C, and 410 to 540 °C, respectively. There is a total loss of about 57.7%, 31.9% and 72.5% for **P-1**, **P-2** and **P-2′** when heated to 750 °C. **P-3** shows a one-step degradation at the beginning temperatures of 410 °C, and tends to complete decomposition at 580 °C. There is a total loss of about 56.2% when heated to 750 °C.

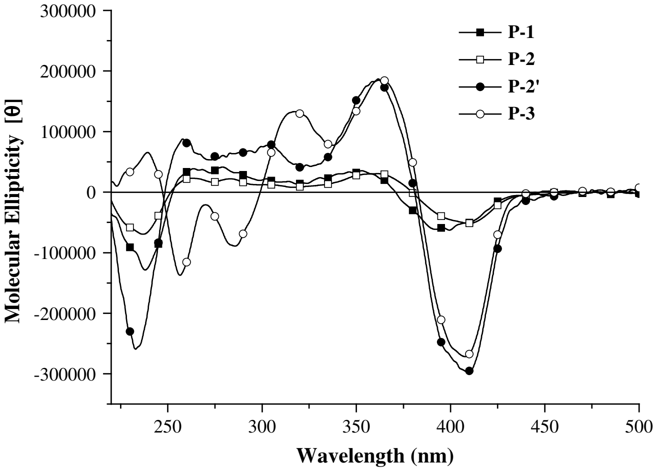

Fig. 4. CD spectra of the repeating units and **P-1**, **P-2**, **P-2′** and **P-3**.

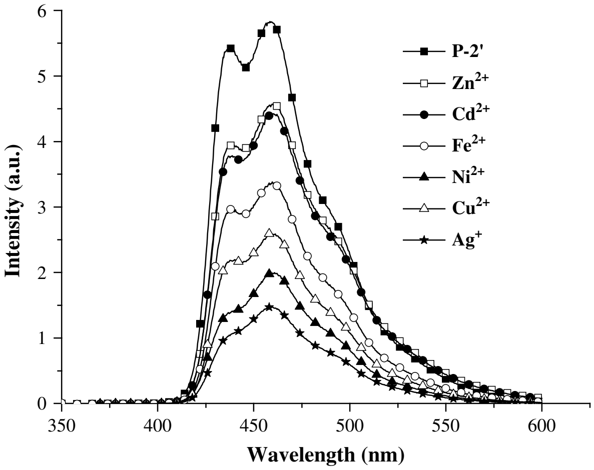

Fig. 5. Emission spectra of metal–polymer complexes for **P-2′** at the ratio of 1:1 (λ_{ex} = 345 nm).

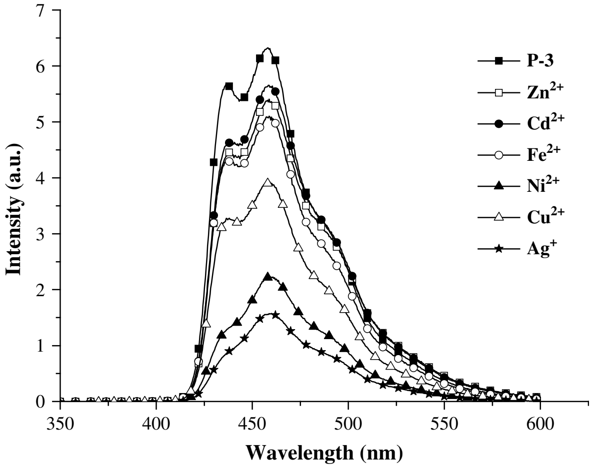

Fig. 6. Emission spectra of metal–polymer complexes for **P-3** at the ratio of 1:1 (λ_{ex} = 342 nm).

3.3. Optical properties

Optical properties of the model compounds **M-1**, ***R*-1**, ***R*-2** and **P-1**, **P-2**, **P-2′**, **P-3** are summarized in Table 2, and Fig. 2 illustrates the

Table 4
The quenching ratio (%) and average lg *K*sv of **P-2′** on metal ions.

	$n_{Polymer}$:n_{ion}								lg K_{SV}[a]
	1:0.2	1:0.4	1:0.6	1:0.8	1:1	1:2	1:3	1:5	
Zn^{2+}	4.45	10.5	14.2	15.4	16.4	19.5	20.6	25.6	3.42
Cd^{2+}	2.91	8.10	15.0	17.5	19.1	25.0	27.5	32.2	3.52
Fe^{2+}	8.58	19.1	27.4	35.7	42.4	54.7	63.6	73.4	4.02
Ni^{2+}	17.7	31.5	44.3	58.3	67.5	90.0	96.0	99.9	4.77
Cu^{2+}	17.3	27.3	40.9	49.5	56.2	67.0	77.8	92.4	4.26
Ag^{+}	23.2	51.1	69.6	71.9	76.2	84.9	88.3	89.4	4.96

[a] Determined upon the molar ratio addition of metal ions for **P-2′** from 1:0.2 to 1:2.

Table 5
The quenching ratio (%) and average lg *K*sv of **P-3** on metal ions.

	$n_{\text{Polymer}}:n_{\text{ion}}$								lg K_{SV}[a]
	1:0.2	1:0.4	1:0.6	1:0.8	1:1	1:2	1:3	1:5	
Zn^{2+}	3.32	5.43	7.46	8.58	9.57	10.0	10.1	10.5	3.11
Cd^{2+}	1.54	3.09	4.21	5.38	7.42	7.57	7.68	7.93	2.95
Fe^{2+}	3.45	6.68	9.97	14.1	18.5	35.7	48.0	60.5	3.62
Ni^{2+}	21.2	34.7	47.9	55.2	67.9	81.9	94.6	99.6	4.54
Cu^{2+}	9.87	18.5	25.8	33.2	38.2	48.4	60.5	81.9	3.92
Ag^{+}	32.9	54.4	67.1	73.6	77.1	85.7	86.7	87.8	4.73

[a] Determined upon the molar ratio addition of metal ions for **P-3** from 1:0.2 to 1:2.

UV–vis absorption spectra of these compounds. According to Fig. 2, UV–vis spectra of the polymers **P-1**, **P-2**, **P-2′** and **P-3** are similar due to the similar repeating units of the polymer backbone. UV–vis absorption maxima λ_{max} of ***R*-1**, ***R*-2** and **M-1** appeared at 240, 268 and 321 nm, and the conjugated polymers **P-1**, **P-2**, **P-2′** and **P-3** in THF show the strong and broad absorption at the region from 350 to 450 nm. Especially, the strongest absorption wavelengths λ_{max} of **P-1**, **P-2**, **P-2′** and **P-3** in THF solution display great red shifts compared to the model compounds ***R*-1**, ***R*-2** and **M-1**, and appear at 373, 383, 384 and 384 nm, respectively. A large red shift in the electronic absorptions of the chiral polymers can be attributed to the effective π–π^* conjugated segment of the linker conjugated units ***R*-1** or ***R*-2** and 2,2′-bipyridyl group *via* vinylene bridge along the main-chain backbone [21,63,64].

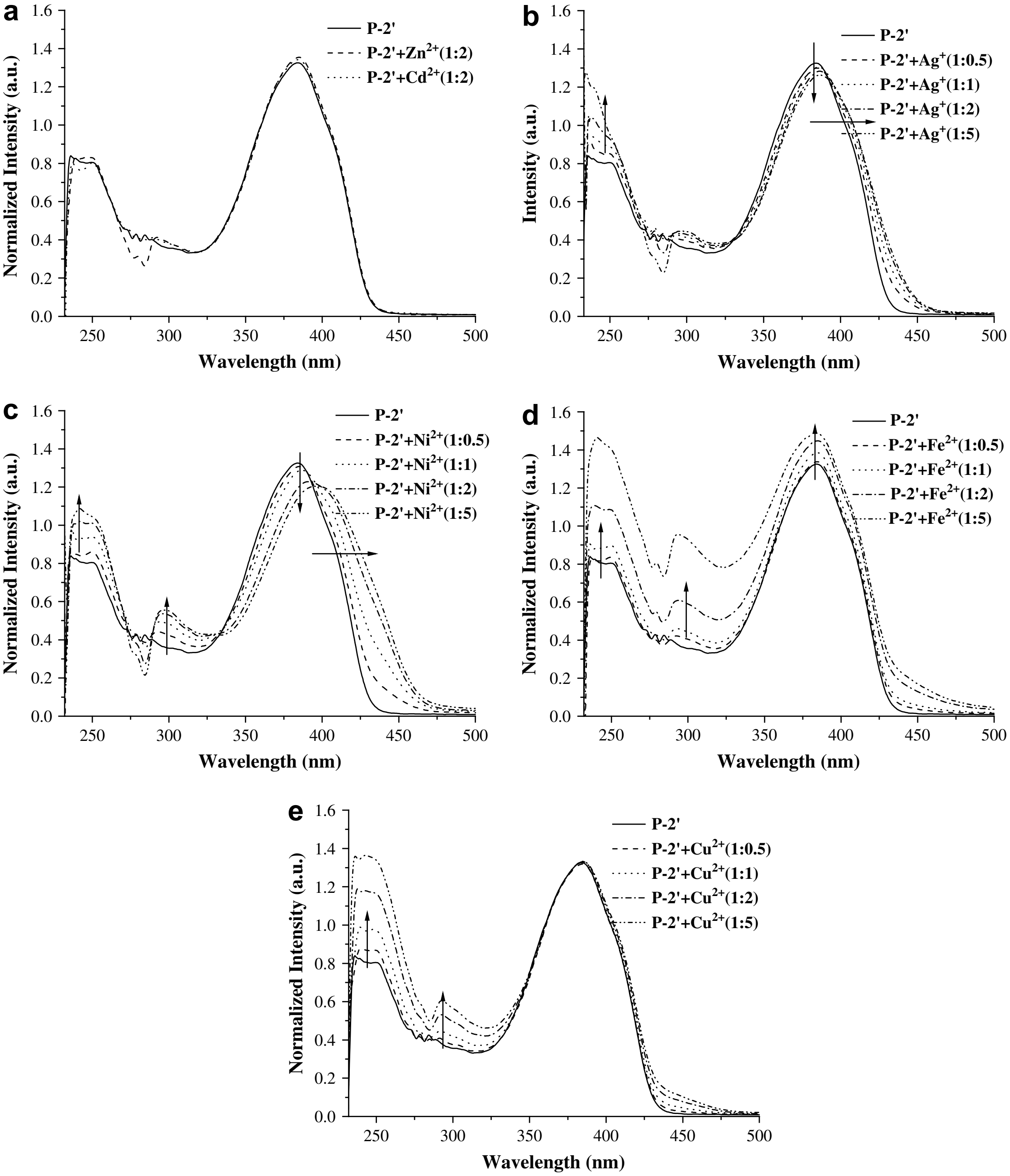

Fig. 7. UV–vis spectra of **P-2′** on Zn^{2+}, Cd^{2+} (a), Ag^{+} (b), Ni^{2+} (c), Fe^{2+} (d) and Cu^{2+} (e).
]

Fluorescence spectra of **M-1**, ***R*-1**, ***R*-2** and **P-1**, **P-2**, **P-2′**, **P-3** are shown in Fig. 3. The four conjugated polymers **P-1**, **P-2**, **P-2′** and **P-3** can emit blue-green light under ultraviolet light (361 nm) or sunlight even in low concentration (1×10^{-4} mol L^{-1}). ***R*-1**, ***R*-2** and **M-1** do not show fluorescence in visible light region. According to Fig. 3, although **P-1**, **P-2** and **P-2′** have the same structure and composition, they have different fluorescent emission spectra. **P-1** and **P-2′** show two wavelength bands at 434 and 455 nm, 437 and 460 nm, respectively, but **P-2** only shows one wavelength band at 458 nm. The fluorescent spectrum of **P-3** is similar to those of **P-1** and **P-2′** and shows two wavelength bands at 437 and 458 nm. The **PL** efficiency (Φ_{PL}) of **P-1**, **P-2**, **P-2′** and **P-3** are 0.50, 0.35, 0.43 and 0.45, respectively. Polymers show strong blue-green fluorescence with high Φ_{PL} due to the extended π-electronic structure between the chiral repeating unit and the conjugated linker unit *via* vinylene bridge [18,19,28]. The greatly enhanced fluorescence of chiral conjugated polybinaphthyls is expected to have the potential application in the polarized light-emitting materials and fluorescent chemosensor on the sensitivity in metal ions sensing.

3.4. CD spectra

The specific rotation values ($[\alpha]_D^{25}$) of the chiral monomers ***R*-M-1**, ***R*-M-2** and ***R*-M-3** are −17.9 (*c* 0.73, THF), −17.7 (*c* 0.62, THF), −56.4 (*c* 0.50, THF), and those of the chiral model compounds ***R*-1** and ***R*-2** are −20.4 (*c* 0.54, THF) and −69.9 (*c* 0.54, THF). $[\alpha]_D^{25}$ of their conjugated polymers **P-1**, **P-2**, **P-2′** and **P-3** are −236.8, −158.3, −758.4 and −410.6 in THF, respectively. CD spectral data of ***R*-1**, ***R*-2**, **P-1**, **P-2**, **P-2′** and **P-3** in THF are summarized in Table 3 and Fig. 4 illustrates the CD spectra of these polymers. The chiral polymers **P-1** and **P-2** exhibit similar intense CD signals with negative and positive Cotton effects in their CD spectra. But their CD signals of Cotton effect at long wavelengths become weak. The optical rotations of **P-1** and **P-2** are a little larger than those of their model compound and monomers, and CD spectra of **P-1** and **P-2** are close to their chiral model compound ***R*-1**. According to Pu's report, if polymer does not have a propagating helical chain conformation in solution, the optical rotation and CD spectrum of this polymer are very close to those of its monomeric model compound. That is, each unit in the polymer acts independently without an organized helical chain structure even though the 1,1′-binaphthyl unit itself is helical [16]. Herein, **P-1** and **P-2** may mainly form a zigzag chain configuration. In contrast to **P-1** and **P-2**, **P-2′** and **P-3** show the strongest CD signals at about 409 nm, and it also can be found $[\alpha]_D^{25}$ of the chiral polymers **P-2′** and **P-3** greatly fluctuate to −758 and −411 and are much larger than those of ***R*-1**, ***R*-2**, **P-1** and **P-2**. According to our previous report [40], the strongest and longest wavelengths of **P-2′** and **P-3** CD spectra appear could be attributed to the helical configuration backbone of the conjugated polymer chains, which is also consistent with their specific rotations. Based on the generation of a helical structure for significant chiral amplification, the results demonstrate **P-2′** and **P-3** could form a helical chain backbone [40,62,65]. According to Pu and Nelson's report [16,66], the molecular weight of the chiral polybinaphthyl had a great influence on the formation of helical configuration. They thought that a higher molecular weight can force the chiral polymer to adopt a helical chain structure. In this paper, we can also find that **P-2′** and **P-3** have higher molecular weight than **P-1** and **P-2**. The formation of the stable helical configuration of **P-2′** and **P-3** can be ascribed to the higher molecular weight. In addition, ^1B_b bands of **P-1**, **P-2** and **P-2′** appear at 238, 237 and 233 nm, and their ^1L_a bands appear at 264, 263 and 258 nm, respectively. On the contrary, **P-3** has the reversed ^1B_b and ^1L_a band signals. This difference may be attributed to the introduction of trifluoromethylphenyl units at 6,6′-positions of 1,1′-binaphthyl. With respect to the chiral polymers, both ^1B_b and ^1L_a bands of ***R*-1** are stronger than those of the corresponding polymers **P-1**, **P-2** and **P-2′**, but the chiral polymers show great red shifts for the ^1B_b and ^1L_a bands. In contrast, CD spectrum of **P-3** shows about 13 nm red shift for ^1B_b band, and no change for ^1L_a band, but appears the reversed signal compared to ***R*-2**. We also found that **P-2′** and **P-3** have stronger Cotton effect at 362 and 363 nm, which can be regarded as the extended conjugated structure in the repeating unit and a high rigidity of polymer backbone [56,59,67,68]. But **P-1** and **P-2** show weaker signs at 353 and 362 nm.

3.5. Responsive signal changes of the conjugated polymer on metal ions

The fluorescence quenching behaviors of the conjugated polymers **P-2′** and **P-3** on transition metal ions were examined in THF solution (Figs. 5 and 6). The influences of various metal ions on the fluorescence emission response of the polymers **P-2′** and **P-3** are shown in Tables 4 and 5. The concentrations of polymers **P-2′** and **P-3** were fixed at 6.0×10^{-5} mol L^{-1} corresponding to 2,2′-bipyridyl receptor units. Zn^{2+}, Cd^{2+}, Fe^{2+}, Ni^{2+}, Cu^{2+} and Ag^{+} ions were used at a concentration of 5.0×10^{-3} mol L^{-1}. Fluorescence quenching behavior of **P-2′** and **P-3** with various molar ratios of transition metal salts was also investigated to examine the effect of the chelating ability on the fluorescence quenching properties of

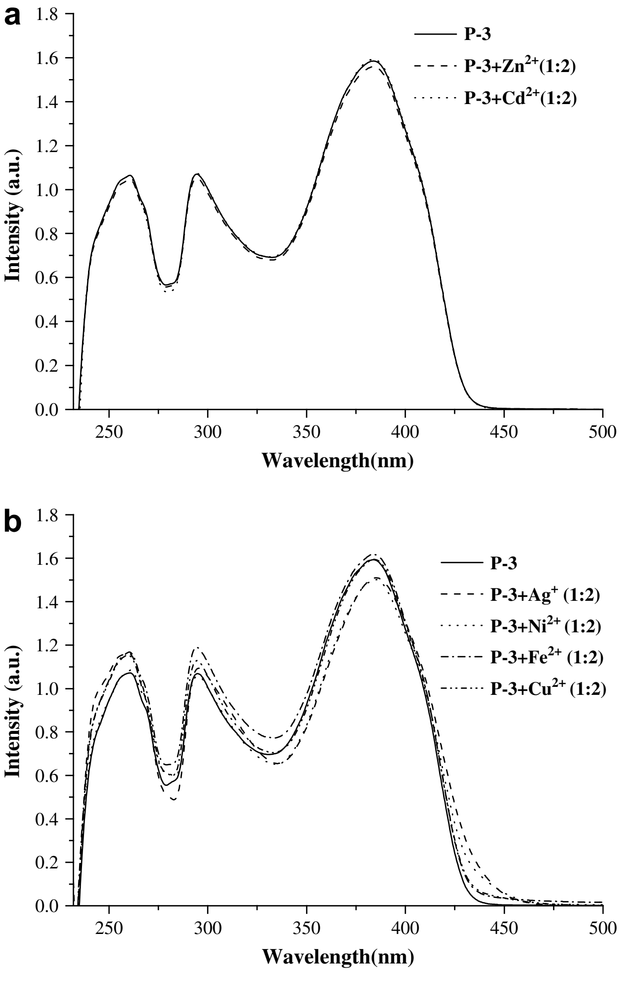

Fig. 8. UV–vis spectra of **P-3** on Zn^{2+}, Cd^{2+} (a), Ag^{+}, Ni^{2+}, Fe^{2+} and Cu^{2+} (b).

the 2,2′-bipyridyl group in polymers. The quenching efficiency is related to the Stern–Volmer constant, K_{SV}, and is determined by monitoring measurable changes in the fluorescence spectra *via* the Stern–Volmer equation: $I_0/I = 1 + K_{SV}[Q]$. Herein, I_0 is the fluorescence emission intensity in the absence of the quencher, and I is the fluorescence emission intensity in the presence of the quencher. $[Q]$ is the quencher concentration, that is transition metal ion concentration. In this paper, the quenching ratios (η) of the polymer to different transition metal ions can be calculated according to equation: $\eta = 1 - I/I_0$. As a result, the fluorescence quenching ratios of **P-2′** are 16.4, 19.1, 42.4, 67.5, 56.2 and 76.2% by Zn^{2+}, Cd^{2+}, Fe^{2+}, Ni^{2+}, Cu^{2+} and Ag^+ upon the 1:1 molar ratio addition of a metal salt solution, while those of **P-3** are 9.57, 7.42, 18.5, 67.9, 38.2 and 77.1%, respectively. Average $\lg K_{SV}$ of the polymer **P-2′** on Zn^{2+}, Cd^{2+}, Fe^{2+}, Ni^{2+}, Cu^{2+} and Ag^+ is 3.42, 3.52, 4.02, 4.77, 4.26 and 4.96, and those of **P-3** are 3.11, 2.95, 3.62, 4.54, 3.92 and 4.73 upon the molar ratio addition of metal ions for polymers from 1:0.2 to 1:2, which shows that **P-2′** has the better sensitivity of these transition metal ions than **P-3**. As is evident from Tables 4 and 5, a slight fluorescence quenching could be detected upon the addition of Zn^{2+} or Cd^{2+}, but Fe^{2+} and Cu^{2+} lead to obvious fluorescence quenching, whereas Ag^+ and Ni^{2+} lead to nearly complete quenching for the two polymers on the ion addition at a concentration of 2:1 molar ratio, which can be attributed to the intramolecular photoinduced electron transfer (PET) or photoinduced charge transfer (PCT) between the polymer backbones and binding metal complexes [69–72]. Herein, metal ions with an open shell electronic structure, which generally show the strong metal–ligand orbital interaction to form low-lying ligand-to-metal (LM) charge transfer state, may exhibit a highly quenching response as in the case of Fe^{2+} with $3d^6$, Ni^{2+} with $3d^8$ and Cu^{2+} with $3d^9$ electronic structure. Metal ions with a full-occupancy outer-shell orbital or half occupancy outer-shell orbital, which generally show the weak metal–ligand orbital interaction, may exhibit a low quenching response as in the case of Zn^{2+} ($3d^{10}$) and Cd^{2+} ($4d^{10}$). But Ag^+ ($4d^{10}$) also causes excellent quenching effect. The observed optical ion-responsive properties are, to a certain degree, ion dependent. The dependence of the response may be associated with metal ion size, coordinating ability with 2,2′-bipyridyl, redox properties, etc. [73].

The UV–vis responses of the conjugated polymers **P-2′** and **P-3** on transition metal ions were tested in THF solution (Figs. 7 and 8). As a result, UV–vis spectra of the polymers appear little change upon the various molar ratio additions of Zn^{2+} and Cd^{2+} for **P-2′** and **P-3** from 1:0.5 to 1:2 (Figs. 7(a) and 8(a)). In contrast, titration curves of UV–vis of **P-2′** and **P-3** exhibit obvious changes as the increasing concentration of Ag^+, Ni^{2+}, Fe^{2+} and Cu^{2+}. For instance, the intensity of UV–vis absorption maxima of the Ag^+–**P-2′** and Ni^{2+}–**P-2′** show the gradual reduction, and the absorption wavelength arising from the conjugated structure of the polymer main-chain backbone appears the gradual red shift from 384 to 387 nm, 384 to 396 nm, respectively, upon the molar ratio additions from 1:0.5 to 1:5, whereas, the absorption peaks of Ag^+–**P-2′** and Ni^{2+}–**P-2′** at 236 nm which is regarded as the absorption band of the naphthyl group show a gradual enhancement relative to the free-metal polymer as the increasing concentration of ion addition (Fig. 7(b) and (c)). Moreover, UV–vis spectra of Cu^{2+}–**P-2′** complex only appears a gradual enhancement of the absorption intensity at 236 nm (Fig. 7(e)), while the absorption intensities of UV–vis spectra of Fe^{2+}–**P-2′** at 236 nm and 384 nm show pronounced

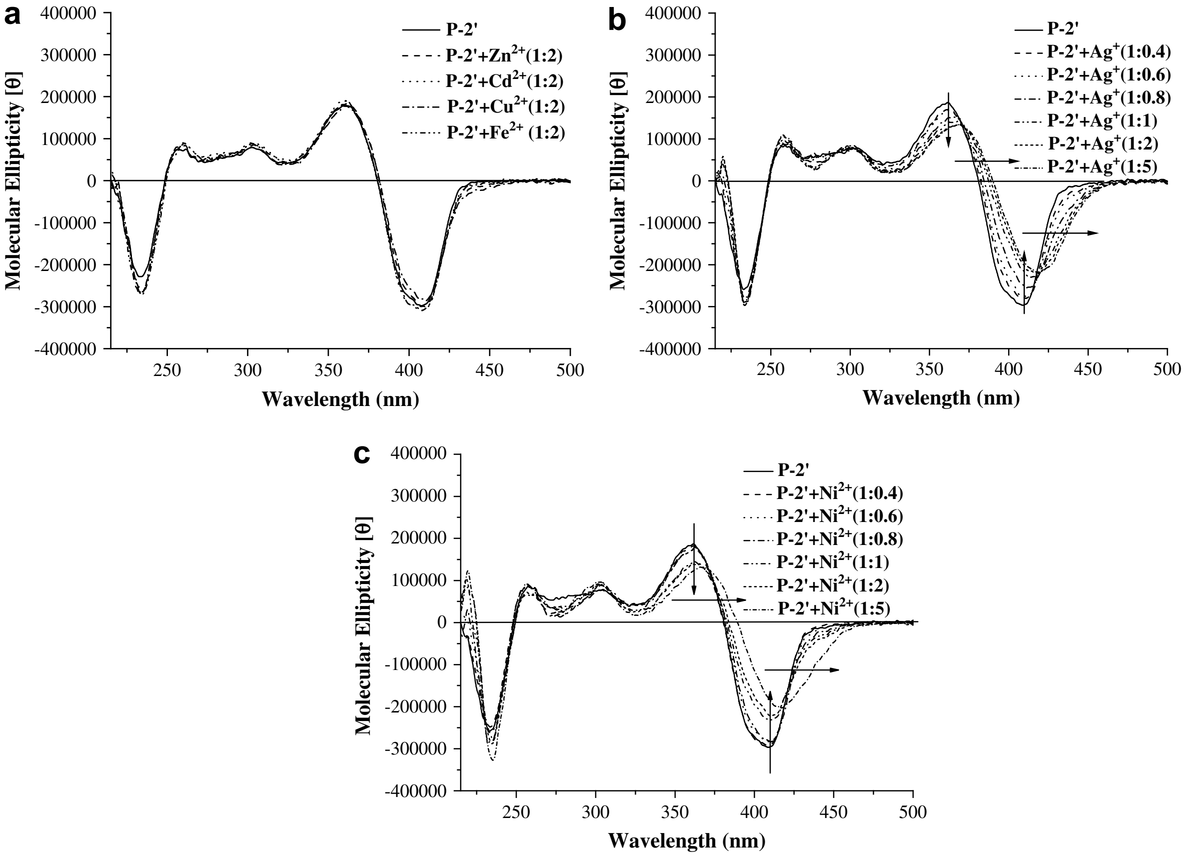

Fig. 9. CD spectra of **P-2′** on Zn^{2+}, Cd^{2+}, Cu^{2+}, Fe^{2+} (a), Ag^+ (b) and Ni^{2+} (c).

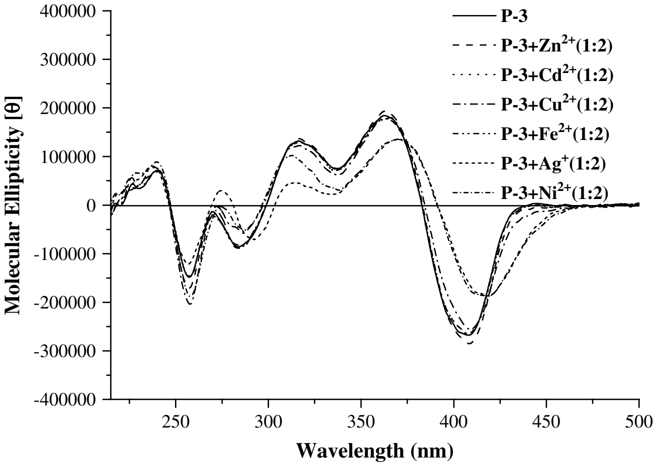

Fig. 10. CD spectra of **P-3** on Zn^{2+}, Cd^{2+}, Cu^{2+}, Fe^{2+}, Ag^{+} and Ni^{2+}.

enhancement too (Fig. 7(d)). The changes of the absorption intensity and wavelength of Ag^{+}–**P-3**, Ni^{2+}–**P-3** and Fe^{2+}–**P-3** are similar to those of Ag^{+}–**P-2′**, Ni^{2+}–**P-2′** and Fe^{2+}–**P-2′** (Fig. 8). Based on Wang and Wasielewski's report, the ion-recognition-induced polymers incorporating 2,2′-bipyridyl moiety in the conjugated polymer main chain could exhibit considerable changes depending on the different metal ions presented and the polymers used. As postulated by the authors, the red shifts of the absorption bands could be ascribed to electron density changes caused by the complexation of metal ions or to conformational changes in the polymer's backbone as a result of the chelation. Blue shifts caused by the coordination of specific metal ions could be attributed to a deconjugation effect on the polymer's backbone [73].

The CD responses of the conjugated polymer **P-2′** and **P-3** on transition metal ions were investigated in THF solution. According to Figs. 9 and 10, the tested metal ions could be categorized into two groups: (1) Zn^{2+}, Cd^{2+}, Cu^{2+} and Fe^{2+}, CD spectra of the metal-chelated polymers exhibit a little changes (Figs. 9(a) and 10); (2) Ag^{+} and Ni^{2+}, CD spectra of the metal-chelated polymers appear great changes (Figs. 9(b),(c) and 10). The CD signal intensity of Ni^{2+}–**P-2′** complex at 361.7 nm, which can be regarded as due to the extended conjugated structure in the repeating unit and a high rigidity of polymer backbone, gradually reduces by 29% upon the molar ratio additions from 1:0.5 to 1:5, and the CD signal intensity at 408.8 nm, which can be attributed to the helical configuration backbone of the conjugated polymer chains, also show a similar degree of reduction. In addition, the long wavelength CD effect of metal-chelated polymer appears the gradual red shift from 361.7 nm to 365.8 nm, 408.8 nm to 417.4 nm upon the various molar ratio additions from 1:0.5 to 1:5. The changes of CD spectra of **P-3** upon the addition of transition metal ions are similar to those of **P-2′** (Fig. 10). The result demonstrates that the CD spectra of the two helical polymers show better sensitive to Ag^{+} and Ni^{2+} than the other transition metal ions Zn^{2+}, Cd^{2+}, Cu^{2+} and Fe^{2+}. The obvious CD effect changes also indicate that transition metal ions can coordinate with 2,2′-bipyridyl moiety in the chiral helical polymers and produce an induced circular dichroism (ICD) in the absorption regions of the polymers. A further comparative study on CD spectrum changes of the chiral helical polymers on transition metal ions will be continued in our group.

4. Conclusion

Four chiral polymers incorporating 2,2′-bipyridyl moieties in the polymer main-chain backbone were synthesized by Heck or Wittig–Horner reaction under different conditions. Based on the great differences of specific rotation values, molecular weight and CD spectra, **P-1** and **P-2** obtained by Heck and Wittig–Horner reaction in the presence of EtONa may adopt a zigzag form, but both **P-2′** and **P-3** synthesized by Wittig–Horner reaction using NaH as a base may exist in a helical configuration. The four polymers have strong blue-green fluorescence due to the extended π-electronic structure between the chiral repeating unit and the conjugated linker 2,2′-bipyridyl group *via* vinylene bridge. Based on the responsive optical properties of the two helical polymers on transition metal ions, Ag^{+} and Ni^{2+} lead to nearly complete fluorescent quenching of the two polymers, Cu^{2+} and Fe^{2+} can cause obvious fluorescence quenching, but Zn^{2+} and Cd^{2+} can only cause slight fluorescence quenching. Ag^{+}, Ni^{2+}, Cu^{2+} and Fe^{2+} could also lead to the obvious changes of UV–vis spectra of the two polymers. On the contrary, Zn^{2+} and Cd^{2+} caused little changes. The CD intensity and wavelength of the chiral polymers also exhibit pronounced changes upon addition of Ag^{+} and Ni^{2+}. The results demonstrate that the 2,2′-bipyridyl moiety in the chiral polymer main-chain backbone can act as the recognition site of a special chemosensor for sensitive detection of transition metal ions.

Acknowledgement

This work was supported by the National Natural Science Foundation of China (No. 20774042) and the Scientific Research Fund of Zhejiang Provincial Education Department (No. 20051292).

References

[1] Brédas JL, Beljonne D, Coropceanu V, Cornil J. Chem Rev 2004;104:4971–5003.
[2] Yu WL, Meng H, Pei J, Huang W, Li YF, Heeger AJ. Macromolecules 1998;31:4838–44.
[3] Kulkarni AP, Zhu Y, Jenekhe SA. Macromolecules 2005;38:1553–63.
[4] McQuade DT, Pullen AE, Swager TM. Chem Rev 2000;100:2537–74.
[5] Thomas III SW, Joly GD, Swager TM. Chem Rev 2007;107:1339–86.
[6] Schubert US, Eschbaumer C. Angew Chem Int Ed 2002;41:2892–926.
[7] Jiang HJ, Gao ZQ, Liu F, Ling QD, Wei W, Huang W. Polymer 2008;49:4369–77.
[8] Liu Z, Zou J, Chen J, Huang L, Peng J, Cao Y. Polymer 2008;49:1604–10.
[9] Hwang SW, Chen Y. Macromolecules 2002;35:5438–43.
[10] Zhan XW, Liu YQ, Wu X, Wang S, Zhu DB. Macromolecules 2002;35:2529–37.
[11] Peng Z, Bao Z, Galvin ME. Adv Mater 1998;10:680–4.
[12] Zhou G, Cheng Y, Wang L, Jing X, Wang F. Macromolecules 2005;38:2148–53.
[13] Li Z, Lou X, Yu H, Li Z, Qin J. Macromolecules 2008;41:7433–9.
[14] Zeng Q, Cai P, Li Z, Qin J, Tang BZ. Chem Commun 2008:1094–6.
[15] Pu L. Chem Rev 2004;104:1687–716.
[16] Zhang HC, Pu L. Macromolecules 2004;37:2695–702.
[17] Li Z, Pu L. Org Lett 2004;6:1065–8.
[18] Liu Y, Zhang S, Miao Q, Zheng L, Zong L, Cheng Y. Macromolecules 2007;40:4839–47.
[19] Liu Y, Miao Q, Zhang S, Huang X, Zheng L, Cheng Y. Macromol Chem Phys 2008;209:685–94.
[20] Liu Y, Zong L, Zheng L, Wu L, Cheng Y. Polymer 2007;48:6799–807.
[21] Pu L. Chem Rev 1998;98:2405–94.
[22] Pu L, Yu HB. Chem Rev 2001;101:757–824.
[23] Fan QH, Li YM, Chan ASC. Chem Rev 2002;102:3385–466.
[24] Xu MH, Lin J, Hu QS, Pu L. J Am Chem Soc 2002;124:14239–46.
[25] Wu L, Zheng L, Zong L, Xu J, Cheng Y. Tetrahedron 2008;64:2651–7.
[26] Huang X, Wu L, Xu J, Zong L, Hu H, Cheng Y. Tetrahedron Lett 2008;49:6823–6.
[27] Deussen HJ, Hendrickx E, Boutton C, Krog D, Clays K, Bechgaard K, et al. J Am Chem Soc 1996;118:6841–52.
[28] Zheng L, Urian RC, Liu Y, Jen AKY, Pu L. Chem Mater 2000;12:13–5.
[29] Li ZB, Pu L. J Mater Chem 2005;15:2860–4.
[30] Koeckelberghs G, Verbiest T, Vangheluwe M, De Groof L, Asselberghs I, Picard I, et al. Chem Mater 2005;17:118–21.
[31] Koeckelberghs G, Vangheluwe M, Picard I, De Groof L, Verbiest T, Persoons A, et al. Macromolecules 2004;37:8530–7.
[32] Bian Z, He YB, Gao LX. Chem J Chin Univ 2004;25:194–6.
[33] Bian Z, He YB, Gao LX. Chem J Chin Univ 2003;24:559–61.
[34] Lam JWY, Tang BZ. Acc Chem Res 2005;38:745–54.
[35] Yashima E, Maeda K. Macromolecules 2008;41:3–12.
[36] Yashima E, Maeda K, Furusho Y. Acc Chem Res 2008;41:1166–80.
[37] Kondo F, Takahashi D, Kimura H, Takeishi M. Polym J 1998;30:161–2.
[38] Nakano T, Okamoto Y. Chem Rev 2001;101:4013–38.

[39] Cornelissen JJLM, Rowan AE, Nolte RJM, Sommerdijk NAJM. Chem Rev 2001;101:4039–70.
[40] Cheng Y, Song J, Zou X, Zhang S, Liu Y, Huang H. Polymer 2006;47:6598–605.
[41] Cheng Y, Zou X, Zhu D, Zhu T, Liu Y, Zhang S, et al. J Polym Sci Part A Polym Chem 2007;45:650–60.
[42] Ishitani H, Ueno M, Kobayashi S. J Am Chem Soc 2000;122:8180–6.
[43] Zhang S, Liu Y, Huang H, Zheng L, Wu L, Cheng Y. Synlett 2008;6:853–6.
[44] Liu B, Yu WL, Pei J, Liu SY, Lai YH, Huang W. Macromolecules 2001;34:7932–40.
[45] Peng Z, Gharavi AR, Yu L. J Am Chem Soc 1997;119:4622–32.
[46] Bougauchi M, Watanabe S, Arai T, Sasai H, Shibasaki M. J Am Chem Soc 1997;119:2329–30.
[47] DiMauro EF, Kozlowski MC. Org Lett 2001;3:1641–4.
[48] Zhang HC, Huang WS, Pu L. J Org Chem 2001;66:481–7.
[49] Belokon YN, Chusov D, Borkin DA, Yashkina LV, Bolotov P, Skrupskaya T, et al. Tetrahedron Asymmetry 2008;19:459–66.
[50] Tsang WCP, Schrock RR, Hoveyda AH. Organometallics 2001;20:5658–69.
[51] Minatti A, Dötz KH. Tetrahedron Asymmetry 2005;16:3256–67.
[52] Sellner H, Faber C, Rheiner PB, Seebach D. Chem Eur J 2000;6:3692–705.
[53] Wang X, Wang X, Guo H, Wang Z, Ding K. Chem Eur J 2005;11:4078–88.
[54] Li ZB, Lin J, Zhang HC, Sabat M, Hyacinth M, Pu L. J Org Chem 2004;69:6284–93.
[55] Kato SI, Takagi K, Suzuki K, Kinoshita T, Yuki Y. J Polym Sci Part A Polym Chem 2004;42:2631–9.
[56] Davey AP, Drury A, Maier S, Byrne HJ, Blau WJ. Synth Met 1999;103:2478–9.
[57] Dalton AB, Coleman JN, in het Panhuis M, McCarthy B, Drury A, Blau WJ, et al. J Photochem Photobiol A Chem 2001;144:31–41.
[58] Cheng Y, Chen L, Song J, Zou X, Liu T. Polym J 2005;37:355–62.
[59] Song J, Cheng Y, Chen L, Zou X, Wang Z. Eur Polym J 2006;42:663–9.
[60] Ma L, Hu QS, Vitharana D, Wu C, Kwan CMS, Pu L. Macromolecules 1997;30:204–18.
[61] Chow HF, Ng MK. Tetrahedron Asymmetry 1996;7:2251–62.
[62] Yashima E, Maeda K, Nishimura T. Chem Eur J 2004;10:42–51.
[63] Cheng Y, Chen L, Zou X, Song J, Wang Z. Polymer 2006;47:435–40.
[64] Meng Y, Slaven IV WT, Wang D, Liu TJ, Chow HF, Li CJ. Tetrahedron Asymmetry 1998;9:3693–707.
[65] Qu J, Suzuki Y, Shiotsuki M, Sanda F, Masuda T. Polymer 2007;48:4628–36.
[66] Nelson JC, Saven JG, Moore JS, Wolynes PG. Science 1997;277:1793–6.
[67] Cheng H, Ma L, Hu QS, Zheng XF, Aderson J, Pu L. Tetrahedron Asymmetry 1996;7:3083–6.
[68] Cheng H, Pu L. Macromol Chem Phys 1999;200:1274–83.
[69] Kokil A, Yao P, Weder C. Macromolecules 2005;38:3800–7.
[70] Kimura M, Horai T, Hanabusa K, Shirai H. Adv Mater 1998;10:459–62.
[71] Murphy CB, Zhang Y, Troxler T, Ferry V, Martin JJ, Jones WE. J Phys Chem B 2004;108:1537–43.
[72] Chen LX, Jäger WJH, Gosztola DJ, Niemczyk MP, Wasielewski MR. J Phys Chem B 2000;104:1950–60.
[73] Wang B, Wasielewski MR. J Am Chem Soc 1997;119:12–21.